Event-Triggered Consensus Control for Networked Underactuated Robotic Systems

Xiang-Yu Yao, Ju H. Park, *Senior Member, IEEE*, Hua-Feng Ding, and Ming-Feng Ge, *Member, IEEE*

***Abstract*—In this article, the consensus of networked underactuated robotic systems subject to fixed and switched communication networks is discussed by developing some novel event-triggered control algorithms, which can synchronously guarantee the convergence of the active states, the boundedness of the velocities of passive actuators, and the exclusion of Zeno behaviors. In the cases of fixed networks, the sufficient criteria are established for the presented distributed event-triggered mechanisms with and without using neighbors' velocities, in order to achieve a better tradeoff between the communication load and system performance. Besides, in the situation of switched networks, the sufficient criterion is established by assuming that the union of the network has a spanning tree. A distributed sampled-data rule is constructed to decide when to update its own and neighbors' estimated positions, and thus further reduces the unnecessary control cost. Finally, by further extending the main results to three other sampled-data control algorithms, several examples with performance comparisons are provided to validate the efficiency and advantages of the theoretical results.**

***Index Terms*—Event-triggered control (ETC), sampled-data communication, switched networks, underactuated robotic systems.**

I. Introduction

During the past few years, researchers from the automatic control community have put a tremendous amount of effort into consensus control of networked systems, which has already become a significant cooperative control topic aiming to force the states of the individuals to reach an agreement [1]–[9]. In many real-world applications, there usually exist a large number of individuals in a networked system in the presence of a restricted bandwidth, limited resources, and a complex control environment. It thus leads to performance degradation or even instability.

Compared with the fully actuated systems, the underactuated systems with fewer active actuators require fewer control inputs, while providing more operation flexibility, and have been widely utilized in many practical applications, including wheeled robots, underwater vehicles, helicopters, and spacecraft [10]–[13]. However, these systems are more complicated and, thus, cannot be controlled and analyzed following the methods of the fully actuated ones, due to the existence of passive actuators, and the strong couplings among the active and passive states. These characteristics will lead to challenging restrictions on stabilizing the system states in an energy-saving manner. In addition, the other inevitable practical system constraints, for example, bandwidth limitation, switched networks, uncertainties, and disturbances [14], [15], will negatively affect the system performance and make the corresponding control problems more challenging.

Event-triggered control (ETC), which can generally provides the tradeoff between the control cost and the system performance, has attracted a large amount of interest in regulating the consensus behaviors of networked systems [16]–[21]. Furthermore, references [22]–[24] concentrated on asynchronous $\mathcal{H}_\infty$ consensus of the Markov jump systems or T–S fuzzy systems with the aim of synthesizing ETC mechanisms to release communication burdens. In [25], the finite-time consensus of systems with single-integrator dynamics and fixed topology was explored by constructing an event-driven finite-time control protocol. Yan *et al.* [26] designed an $\mathcal{H}_\infty$ ETC algorithm for networked systems with distributed channel delay. The technical note [27] adopted output-feedback and back stepping techniques for the ETC problem with both unknown control direction and sensor faults while for the consensus of underactuated systems, Postoyan *et al.* [28] presented emulation-like ETC methods for stabilizing time-varying tracking of unicycle mobile robots, and Xu *et al.* [29] proposed an ETC-based adaptive fuzzy sliding-mode control approach for switched underactuated systems. Moreover, some other ETC results with the model predictive control [30], backstepping control [31], and neural network control [32] have been obtained. However, all of the above results still need continuous-time communication, resulting in large energy consumption.

As a matter of fact, the communications in practical applications generally proceed over digital networks, and the corresponding networks are always dynamically switched due

Manuscript received March 25, 2020; revised July 5, 2020; accepted September 17, 2020. Date of publication October 23, 2020; date of current version May 19, 2022. This work was supported in part by the National Natural Science Foundation of China under Grant 51975544, Grant 51675495, Grant 62073301, and Grant 61703374; and in part by the Fundamental Research Funds for National Universities, China University of Geosciences (Wuhan). The work of Ju H. Park was supported by the National Research Foundation of Korea grant funded by the Korea Government (MSIT) under Grant 2020R1A2B5B02002002. This article was recommended by Associate Editor C.-Y. Su. *(Corresponding authors: Ju H. Park; Hua-Feng Ding.)*

Xiang-Yu Yao is with the School of Mechanical Engineering and Electronic Information, China University of Geosciences, Wuhan 430074, China, and also with the Department of Electrical Engineering, Yeungnam University, Gyeongsan 38541, South Korea (e-mail: xyyao518@163.com).

Ju H. Park is with the Department of Electrical Engineering, Yeungnam University, Gyeongsan 38541, South Korea (e-mail: jessie@ynu.ac.kr).

Hua-Feng Ding and Ming-Feng Ge are with the School of Mechanical Engineering and Electronic Information, China University of Geosciences, Wuhan 430074, China (e-mail: dinghf@cug.edu.cn; fmgabc@163.com).

Color versions of one or more figures in this article are available at https://doi.org/10.1109/TCYB.2020.3025604.

Digital Object Identifier 10.1109/TCYB.2020.3025604

TABLE I
SOME MAIN SYMBOLS

Symbols	Descriptions
$\mathbb{N},\ \mathbb{Z}^+$	The Natural Number and Positive Integer
$\otimes,\ I_n$	Kronecker Product, $n\times n$ Identity Matrix
$\mathbb{R}^N, \mathbb{R}^{n\times m}$	The $N\times 1$ and $n\times m$ Real Matrices
$\|\|\|_1,\ \|\|\|_2$	1-Norm and 2-Norm (Euclidean Norm)
$\sup, \mathrm{mod}$	The Supremum and Modulo Functions
$\lambda_{\min}, \lambda_{\max}$	Minimum and Maximum Eigenvalues
$q_p, \dot{q}_p, \ddot{q}_p$	Passive States with Subscript p
$q_a, \dot{q}_a, \ddot{q}_a$	Active States with Subscript a
$\tau_a,\ D_a$	Active Control Input and Disturbance
$\mathcal{G}_f,\ \mathcal{L}_f$	The Fixed Communication Networks
$\mathcal{G}_{s_g},\ \mathcal{L}_{s_g}$	Switched Communication Networks
$\omega_{f,ij}, \omega_{s_g,ij}$	The Elements of Adjacency Matrices
x_p, x_a, s_p, s_a	Relative-State and Sliding-Mode Vectors
$\hat{\Omega},\ \hat{H}_{pp}$	Observer and Estimated Inertia Component
$\hat{q}_a(t^k)$	The Sampled-Data Estimated Positions
$F,\ E$	Trigger Function and Measurement Error
$t^k,\ t^{k-1}$	The k-th and $(k-1)$-th Events for $k\in\mathbb{Z}^+$
T^k	The Trigger Time Intervals $T^k = t^k - t^{k-1}$
Y	Regressor $Y=[Y_p^T, Y_a^T]^T$ with Y_p and Y_a
Y_p	Regressor $Y_p = Y_p(q,\dot{q},x_p,\dot{x}_p,x_a,\dot{x}_a)$
Y_a	Regressor $Y_a = Y_a(q,\dot{q},x_p,\dot{x}_p,x_a,\dot{x}_a)$
Y_p^*	Regressor $Y_p^* = Y_p(q,\dot{q},x_p,0_{n_p},x_a,\dot{x}_a)$

to their limitations and unreliability. Therefore, the necessary interconnections adopted in fixed cases may fracture, and the isolated individuals may even occur, which inevitably brings great difficulties for the convergence analysis and control process. In conclusion, the existing results developed with fixed topologies and continuous-time communications cannot be directly extended to deal with such switched cases. For this reason, numerous efforts have been made, for instance, You *et al.* [33] and Yang *et al.* [34] established an output feedback-based ETC frameworks without continuous-time communications for consensus of nonlinear systems subject to actuator saturation or disturbance. The works [35], [36] contributed to form discrete-time sampling ETC schemes for the consensus of first-order and second-order systems. Under sampled-data switched policies, [37] was concerned with the ETC of a class of fuzzy Markov jump systems. Wu *et al.* [38] discussed the consensus ETC of multiagent systems with fixed and switched communication networks. With regard to underactuated systems, Chu *et al.* [39] presented sampled-data ETC methods for the tracking control of nonholonomic systems and Deng *et al.* [40] studied the ETC tracking of an underactuated surface vessel in the sensor-to-controller channel. However, the above results are derived by employing the knowledge of neighbors' velocities, which are not easily available in some practical cases due to the limitations of sensors and other hardware costs. Besides, the involved dynamics of works [39]–[41] are not in the Euler–Lagrange form.

By the aforementioned discussion, there are two main challenges: 1) how to investigate underactuated Euler–Lagrange systems with switched networks and 2) how to develop algorithms without relative full-state feedbacks and continuous-time communications. Motivated to solve these challenges, the authors investigate the ETC-based consensus of underactuated systems. The novelties and contributions compared with the former literature are summarized as follows.

1) Focusing on the nonlinear-networked underactuated Euler–Lagrange systems with internal uncertainties and external disturbances, this article develops several robust ETC algorithms over fixed and switched communication networks, which are capable of keeping satisfied control performances with less control cost.
2) In order to further reduce control cost based on only partial information of neighbors' states, a relative-position filter layer is newly presented to construct effective control algorithms without using neighbors' velocities. Besides, a distributed sampled-data estimator layer driven by the ETC mechanism is designed without requiring neighbors' real positions and continuous-time communications.

The remainder is arranged as follows. Preliminaries and main results are, respectively, provided in Sections II and III. Simulation and conclusion are drawn in Sections IV and V, respectively. Some main symbols are listed in Table I.

II. PRELIMINARIES

A. System Formulation

Consider the following networked underactuated robotic systems with individual set $i \in \{1,\ldots,N\}$:

$$H_i(q_i)\ddot{q}_i + C_i(q_i,\dot{q}_i)\dot{q}_i + C_{fi}(q_i,\dot{q}_i)\dot{q}_i + G_i(q_i) = \tau_i + D_i \quad (1)$$

where $t \in [t_0,\infty)$, $q_i,\dot{q}_i,\ddot{q}_i \in \mathbb{R}^n$ are position, velocity, and acceleration. $H_i(q_i), C_i(q_i,\dot{q}_i), C_{fi}(q_i,\dot{q}_i) \in \mathbb{R}^{n\times n}$, and $G_i(q_i)\in\mathbb{R}^n$ are the positive-definite inertial matrix, Coriolis–centrifugal, damping-friction, and gravitational matrices, and $\tau_i, D_i \in \mathbb{R}^n$ are control input and external disturbance. Note that the system states consist of active states $q_{ia},\dot{q}_{ia},\ddot{q}_{ia}\in\mathbb{R}^{n_a}$ and passive ones $q_{ip},\dot{q}_{ip},\ddot{q}_{ip}\in\mathbb{R}^{n_p}$, with $n_a+n_p=n$, such that there usually exist two classes of structures [13].

Passive–Active Structure: $q_i=[q_{ip}^T,q_{ia}^T]^T$, $\dot{q}_i=[\dot{q}_{ip}^T,\dot{q}_{ia}^T]^T$, $\ddot{q}_i=[\ddot{q}_{ip}^T,\ddot{q}_{ia}^T]^T$, $\tau_i=[0_{ip}^T,\tau_{ia}]^T$, and $D_i=[0_{ip}^T,D_{ia}^T]^T$.

Active–Passive Structure: $q_i=[q_{ia}^T,q_{ip}^T]^T$, $\dot{q}_i=[\dot{q}_{ia}^T,\dot{q}_{ip}^T]^T$, $\ddot{q}_i=[\ddot{q}_{ia}^T,\ddot{q}_{ip}^T]^T$, $\tau_i=[\tau_{ia},0_{ip}^T]^T$, and $D_i=[D_{ia}^T,0_{ip}^T]^T$.

Remark 1: Throughout this article, it is assumed that there are N individuals in system (1) labeled in an ordered sequence $\{1,2,\ldots,N\}$, and each individual consists of passive and active actuators labeled with subscripts p and a, respectively. Thus, the passive states $(q_{ip},\dot{q}_{ip},\ddot{q}_{ip})$, active states $(q_{ia},\dot{q}_{ia},\ddot{q}_{ia})$, and the corresponding control parameters with the subscript p or a can be directly used without confusion.

By selecting different coordinates, we can obtain the following uniform dynamics (2) with relevant common properties [42], whether we study the first structure or the second one

$$\begin{bmatrix} H_{ipp} & H_{ipa} \\ H_{iap} & H_{iaa}\end{bmatrix}\begin{bmatrix}\ddot{q}_{ip}\\ \ddot{q}_{ia}\end{bmatrix} + \begin{bmatrix} C_{ipp} & C_{ipa} \\ C_{iap} & C_{iaa}\end{bmatrix}\begin{bmatrix}\dot{q}_{ip}\\ \dot{q}_{ia}\end{bmatrix} + \begin{bmatrix} C_{fip} & 0_{n_p\times n_a} \\ 0_{n_a\times n_p} & C_{fia}\end{bmatrix}\begin{bmatrix}\dot{q}_{ip}\\ \dot{q}_{ia}\end{bmatrix} + \begin{bmatrix} G_{ip}\\ G_{ia}\end{bmatrix} = \begin{bmatrix} 0_{ip}\\ \tau_{ia}+D_{ia}\end{bmatrix}. \quad (2)$$

Property 1: The dynamic terms in systems (2) are bounded, and for arbitrary vector $Z = [Z_p^T, Z_a^T]^T \in \mathbb{R}^n$, it satisfies

$$Z^T\left(\begin{bmatrix} \dot{H}_{ipp} & \dot{H}_{ipa} \\ \dot{H}_{iap} & \dot{H}_{iaa} \end{bmatrix} - 2\begin{bmatrix} C_{ipp} & C_{ipa} \\ C_{iap} & C_{iaa} \end{bmatrix}\right)Z = 0.$$

Property 2: For arbitrary vectors $Z_1 = [Z_{1p}^T, Z_{1a}^T]^T \in \mathbb{R}^n$ and $Z_2 = [Z_{2p}^T, Z_{2a}^T]^T \in \mathbb{R}^n$, it satisfies

$$\begin{aligned} Y_i\vartheta_i = &\begin{bmatrix} H_{ipp} & H_{ipa} \\ H_{iap} & H_{iaa} \end{bmatrix} Z_1 + \begin{bmatrix} C_{ipp} & C_{ipa} \\ C_{iap} & C_{iaa} \end{bmatrix} Z_2 \\ &+ \begin{bmatrix} C_{fip} & 0_{n_p\times n_a} \\ 0_{n_a\times n_p} & C_{fia} \end{bmatrix} Z_2 + \begin{bmatrix} G_{ip} \\ G_{ia} \end{bmatrix} \end{aligned}$$

where $Y_i = [Y_{ip}^T(q_i, \dot{q}_i, Z_1, Z_2), Y_{ia}^T(q_i, \dot{q}_i, Z_1, Z_2)]^T$, and ϑ_i is the integration with respect to (w.r.t.) system parameters.

Remark 2: Systems with dynamic uncertainties $\hat{\vartheta}_i$ yield

$$\begin{aligned} Y_i\hat{\vartheta}_i = &\begin{bmatrix} \hat{H}_{ipp} & \hat{H}_{ipa} \\ \hat{H}_{iap} & \hat{H}_{iaa} \end{bmatrix} Z_1 + \begin{bmatrix} \hat{C}_{ipp} & \hat{C}_{ipa} \\ \hat{C}_{iap} & \hat{C}_{iaa} \end{bmatrix} Z_2 \\ &+ \begin{bmatrix} \hat{C}_{fip} & 0_{n_p\times n_a} \\ 0_{n_a\times n_p} & \hat{C}_{fia} \end{bmatrix} Z_2 + \begin{bmatrix} \hat{G}_{ip} \\ \hat{G}_{ia} \end{bmatrix}. \end{aligned}$$

B. Mathematical Preparations

For the underactuated system over fixed and switched communication networks, digraphs $\mathcal{G}_f = \{\mathcal{V}, \mathcal{E}, \mathcal{A}_f, \mathcal{L}_f\}$ and $\mathcal{G}_{s_g} = \{\mathcal{V}, \mathcal{E}, \mathcal{A}_{s_g}, \mathcal{L}_{s_g}\}$ are, respectively, introduced with individual set $\mathcal{V} = \{1, \ldots, N\}$ and directed communication edge set $\mathcal{E} = \{\mathcal{E}_{j\to i} | i, j \in \mathcal{V}, i \neq j\}$. Note that subscript s_g represents the switched networks with the switch index $g \in \mathbb{N}$. $\mathcal{A}_f = [\omega_{f,ij}]_{N\times N}$ and $\mathcal{A}_{s_g} = [\omega_{s_g,ij}]_{N\times N}$ are adjacency matrices, where $\omega_{f,ij}, \omega_{s_g,ij} > 0$, if the communication edge $\mathcal{E}_{j\to i}$ is valid, and $\omega_{f,ij}, \omega_{s_g,ij} = 0$ otherwise. $\mathcal{L}_f = [l_{f,ij}]_{N\times N}$ and $\mathcal{L}_{s_g} = [l_{s_g,ij}]_{N\times N}$ are the Laplacian matrices with $l_{f,ii} = \sum_{j=1}^N \omega_{f,ij}$ and $l_{s_g,ii} = \sum_{j=1}^N \omega_{s_g,ij}$, as well as $l_{f,ij} = -\omega_{f,ij}$ and $l_{s_g,ij} = -\omega_{s_g,ij}$ for $i \neq j$. In addition, there is a virtual static leader labeled as 0 for the fixed networks, with a pinning matrix $\mathcal{B} = \mathrm{diag}\{b_1, \ldots, b_i, \ldots, b_N\}$ among the leader and other individuals. Note that $b_i > 0$ if $\mathcal{E}_{0\to i}$ is valid, and $b_i = 0$ otherwise. Then, some related assumptions on the communication networks and control algorithms are proposed as follows.

Assumption 1: The fixed communication network $\mathcal{G}_f$ with the virtual leader across $t \in [t_0, \infty)$ has a spanning tree, namely, the leader has communication edges to any other individuals.

Assumption 2: There exist positive integers g_0 and g_1 such that the union of the switched communication network $\bigcup_{g=g_0}^{g_1} \mathcal{G}_{s_g}$ across $g \in [g_0, g_1]$ has a spanning tree.

Assumption 3: This article studies underactuated system (2) with ETC algorithms, which assumes that the trigger time intervals $T^k = t^k - t^{k-1}$ are bounded by $T^k \leq \bar{T}$, for a positive constant $\bar{T}$, and $k \in \mathbb{Z}^+$.

Assumption 4: By the general boundedness property of the Euler–Lagrange dynamics, assume that the damping-friction matrix in (2) is diagonal positive definite, satisfying $q_{ip}^T C_{fip} q_{ip} \geq g_2 \geq \|C_{ipp}\| q_{ip}^2$, $q_{ia}^T C_{fia} q_{ia} \geq g_3$, $\exists g_2 > 0$, $\exists g_3 > 0$.

Furthermore, the main definitions and lemmas w.r.t. the control problem are presented as follows.

Definition 1: Underactuated system (2) is driven to achieve consensus if the Laplacian matrix $\mathcal{L} \in \{\mathcal{L}_f, \mathcal{L}_{s_g}\}$, and states $q_a = [q_{1a}^T, \ldots, q_{Na}^T]^T$, $\dot{q}_a = [\dot{q}_{1a}^T, \ldots, \dot{q}_{Na}^T]^T$, and $\dot{q}_p = [\dot{q}_{1p}^T, \ldots, \dot{q}_{Np}^T]^T$ satisfy

$$\lim_{t\to\infty} \left\| \left(\mathcal{L} \otimes I_{n_a}\right) q_a(t) \right\| = 0, \quad \lim_{t\to\infty} \|\dot{q}_a(t)\| = 0, \quad \dot{q}_p(t) \in \mathbb{L}_\infty. \tag{3}$$

Definition 2: If there exist infinite trigger numbers in a finite time, it is called the Zeno behavior, which is an undesirable phenomenon costing vast resources, and should be avoided.

Definition 3: The average trigger rate is defined as a performance index that is equal to the average ratio between the actual trigger numbers and total computation numbers of control inputs, and generally, the less the ratio is, the less resource it costs.

Lemma 1 [43]: Consider a twice differentiable system $\dot{x} = f(t, x)$: 1) if $f(t, x), \dot{f}(t, x) \in \mathbb{L}_\infty$, then it concludes $f(\infty, x) \to 0$ and 2) if $f(t, x), \ddot{f}(t, x) \in \mathbb{L}_\infty$, then $\dot{f}(\infty, x) \to 0$.

Lemma 2 [44]: If the leader in the system has directed communication edges to any other individuals, the real parts of eigenvalues of matrix $\mathcal{W} = \mathcal{L}_f + \mathcal{B}$ are all positive.

Lemma 3 [43], [45]: Consider a system $\dot{x}(t) = Ax(t) + Bu(t)$ with state $x(t) \in \mathbb{R}^n$, input $u(t) \in \mathbb{R}^m$, and the Hurwitz matrix A.

1) The system is input-to-state stable with $x(\infty) \to 0$ if it has a globally exponentially stable equilibrium point at origin $x(t) = 0$ with $u(t) = 0$.
2) For any input $u(t) \in \mathbb{L}_\infty$ and initial state $x(t_0) \in \mathbb{R}^n$, the system response over $t \in [t_0, \infty)$ satisfies $\|x(t)\|_2 \leq \exp(-\delta t)\|x(t_0)\|_2 + (\|B\|_2/\delta)\|u(t)\|_2$, $\exists \delta \in \mathbb{Z}^+$.

Lemma 4 [46]: The non-negative matrix $M \in \mathbb{R}^{N\times N}$ is row stochastic if all elements of each row sum are equal to one.

Lemma 5 [47]: For a non-negative matrix $M_g \in \mathbb{R}^N \times \mathbb{R}^N$ with positive diagonal entries, it satisfies $\prod_{g=0}^k M_g \geq \hbar \sum_{g=0}^k M_g$ for $\hbar > 0$ and $k \in \mathbb{Z}^+, k \geq 2$.

Lemma 6 [48]: If a non-negative matrix $M \in \mathbb{R}^{N\times N}$ has the same positive constant row sums given by $\rho > 0$, then ρ is an eigenvalue of M with an associated eigenvector 1_N. In addition, the eigenvalue ρ of M has an algebraic multiplicity equal to one, if and only if the graph associated with M, that is, $\mathcal{G}(M)$, contains a spanning tree.

Lemma 7 [49]: A row stochastic matrix $M \in \mathbb{R}^{N\times N}$ is indecomposable and aperiodic (SIA), if one of the following conditions holds.

1) There exists a constant column vector $y \in \mathbb{R}^N$ satisfying $\lim_{k\to\infty} A^k = 1_N y^T$.
2) The eigenvalues of matrix M are positive, and its digraph $\mathcal{G}(M)$ contains a spanning tree.

Lemma 8 [50]: Let $M_1, M_2, \ldots, M_k \in \mathbb{R}^N \times \mathbb{R}^N$ be a finite set of SIA matrices with the property that for each sequence $M_{i1}, M_{i2}, \ldots, M_{ij}$ with a positive length, the matrix product $M_{i1} M_{i2} \ldots M_{ij}$ is SIA. Then, for each infinite sequence $M_{i1} M_{i2} \ldots M_{ij} \ldots$, there exists a constant column vector $y \in \mathbb{R}^N$ satisfying $\lim_{j\to\infty} M_{i1} M_{i2} \ldots M_{ij} = 1_N y^T$.

Remark 3: Note that the control objective of the article is to guarantee the convergence of the active states $(q_{ia}, \dot{q}_{ia})$, and the boundedness of the velocities $(\dot{q}_{ip})$ of passive actuators simultaneously. On the other hand, it should be pointed out that how to achieve the convergence of the passive states, that is, how to swing the system up to the vertical upward equilibrium point, is an important research topic in the field of the underactuated systems, and we will deeply consider the control problem via ETC algorithms in our future works.

III. Main Results

A. Distributed ETC With Fixed Communication Networks

Under fixed networks, the consensus of systems (2) is achieved through a distributed ETC algorithm, including a relative-state filter layer, an observer-based control layer, and an event-triggered layer. A sliding-mode vector $s_i \in \mathbb{R}^n$ for both active and passive parts is first designed as

$$s_i = \begin{bmatrix} s_{ip} \\ s_{ia} \end{bmatrix} = \begin{bmatrix} \dot{q}_{ip} - x_{ip} \\ \dot{q}_{ia} - x_{ia} \end{bmatrix} \tag{4}$$

where x_{ip}, x_{ia} are derived by relative-state filter layer below

$$\begin{bmatrix} \dot{x}_{ip} \\ x_{ia} \end{bmatrix} = \begin{bmatrix} \hat{H}_{ipp}^{-1}\Big(K_{ip}s_{ip} - Y_{ip}^{*}\hat{\vartheta}_i\Big) \\ -\alpha_i \sum_{j=1}^{N} \omega_{f,ij} q_{ija} - \alpha_i b_i q_{i0a} \end{bmatrix} \tag{5}$$

where $\alpha_i > 0$, $q_{ija} = q_{ia} - q_{ja}$, and $q_{i0a} = q_{ia} - q_{0a}$, with known static state q_{0a} to some individuals, $Y_{ip}^{*} = Y_{ip}(q_i, \dot{q}_i, x_{ip}, 0_{n_p}, x_{ia}, \dot{x}_{ia})$, $\hat{H}_{ipp}$ is an estimated parameter w.r.t. $\hat{\vartheta}_i$, and $\hat{\vartheta}_i$ is generated by the following observer-based control layer

$$\begin{cases} \tau_{ia}(t) = Y_{ia}(t_i^k)\hat{\vartheta}_i(t_i^k) - \hat{K}_{ia}(t_i^k)s_{ia}(t_i^k) - \hat{D}_{ia}(t_i^k) & \text{(6a)} \\ \dot{\hat{\Omega}}_i(t) = \begin{bmatrix} \Gamma_{\vartheta i} & 0 & 0 \\ 0 & \Gamma_{ki} & 0 \\ 0 & 0 & \Gamma_{di} \end{bmatrix} \begin{bmatrix} -Y_i^T(t)s_i(t) \\ s_{ia}^T(t)s_{ia}(t) \\ s_{ia}(t) \end{bmatrix} & \text{(6b)} \end{cases}$$

where $t \in [t_i^k, t_i^{k+1})$, $\hat{\Omega}_i(t) = [\hat{\vartheta}_i^T(t), \hat{K}_{ia}^T(t), \hat{D}_{ia}^T(t)]^T$, $Y_i = [Y_{ip}^T(q_i, \dot{q}_i, x_{ip}, \dot{x}_{ip}, x_{ia}, \dot{x}_{ia}), Y_{ia}^T(q_i, \dot{q}_i, x_{ip}, \dot{x}_{ip}, x_{ia}, \dot{x}_{ia})]^T$, and $\Gamma_{\vartheta i}$, Γ_{ki}, and Γ_{di} are symmetric positive-definite matrices. The update of the control layer is decided by the following event-triggered layer:

$$\begin{cases} F_i = \|E_i\|_1 - \xi_i\|s_{ia}\|_1 + \zeta_i(t) & \text{(7a)} \\ E_i = \begin{bmatrix} -Y_{ia}\big(t_i^k\big)\hat{\vartheta}_i\big(t_i^k\big) + Y_{ia}\hat{\vartheta} \\ \hat{K}_{ia}\big(t_i^k\big)s_{ia}\big(t_i^k\big) - \hat{K}_{ia}s_{ia} \\ \hat{D}_{ia}\big(t_i^k\big) - \hat{D}_{ia} \end{bmatrix} & \text{(7b)} \end{cases}$$

where $\zeta_i(t) = -\varepsilon_i \exp(-\mu_i t)$, $\xi_i, \varepsilon_i > 0$, $\mu_i \in (0, 1)$, and F_i and E_i are the trigger function and measurement error, respectively.

Remark 4: Note that the event-triggered layer satisfies $F_i \leq 0$, and if $F_i = 0$, it triggers and the control layer is updated. Moreover, the update frequency can be adjusted by designing proper parameters ε_i and μ_i, which guarantees an optimal tradeoff between the control cost and performance.

Under fixed communication networks, the developed distributed ETC algorithm and signal flow diagram are displayed in Table II and Fig. 1, respectively.

TABLE II
ALGORITHM I

Algorithm	The Distributed ETC Algorithm over Fixed Communication Networks
Step I	For individual $i \in \mathcal{V}$, initialize the positions and velocities $q_{ip}(t_0), q_{ia}(t_0), \dot{q}_{ip}(t_0), \dot{q}_{ia}(t_0) \in \mathbb{L}_\infty$, relative state and observer $x_{ip}(t_0), \hat{\Omega}_i(t_0) \in \mathbb{L}_\infty$.
Step II	Obtain $x_i(t)$ and $\dot{x}_i(t)$ via the relative-state filter layer with parameters $\hat{H}_{ipp}(t), s_i(t), q_i(t), \dot{q}_i(t)$, $Y_{ip}^*(t), \hat{\vartheta}_i(t), \omega_{f,ij}$ and neighbor's velocity $\dot{q}_j(t)$.
Step III	Achieve $\tau_{ia}(t)$ and $\hat{\Omega}_i(t)$ via the observer-based control layer with x_i, $\dot{x}_i$, s_i, Y_i, $\Gamma_{\vartheta i}$, Γ_{ki}, Γ_{di}.

Step IV	Based on the event-triggered layer with trigger function F_i and measurement error E_i
	For sample time $t \in [t_0, \infty)$
	If $F_i(t) = 0$ at trigger time $t \in \{t_i^k \mid k \in \mathbb{Z}^+\}$
	The control layer at time $t = t_i^k$ is updated
	Else the control layer remain unchanged
	End If
	End For

Theorem 1: For underactuated systems (2) with a fixed network, if Assumption 1 holds, the developed distributed ETC algorithm, shown in Table II, can simultaneously address the asymptotic consensus and the Zeno behavior problems, respectively, proposed in Definitions 1 and 2, that is, $\|(\mathcal{L}_f \otimes I_{n_a})q_a(\infty)\|$, $\|\dot{q}_a(\infty)\| \to 0$, $\dot{q}_p(\infty) \in \mathbb{L}_\infty$, and $T^k = t^k - t^{k-1} > 0$.

Proof: Substituting (4) and (6) into system (2) yields

$$\begin{bmatrix} H_{ipp} & H_{ipa} \\ H_{iap} & H_{iaa} \end{bmatrix}\begin{bmatrix} \dot{s}_{ip} \\ \dot{s}_{ia} \end{bmatrix} = \begin{bmatrix} -Y_{ip}\vartheta_i \\ -Y_{ia}\vartheta_i + D_{ia} + \tau_{ia} \end{bmatrix} - \left\{\begin{bmatrix} C_{fip} & 0_{n_p\times n_a} \\ 0_{n_a\times n_p} & C_{fia} \end{bmatrix} - \begin{bmatrix} C_{ipp} & C_{ipa} \\ C_{iap} & C_{iaa} \end{bmatrix}\right\}\begin{bmatrix} s_{ip} \\ s_{ia} \end{bmatrix}. \tag{8}$$

Then, consider the following Lyapunov-like function candidate with parameters $\tilde{\Omega}_i = \Omega_i - \hat{\Omega}_i$ and $\Gamma_i = \text{diag}\{\Gamma_{\vartheta i}, \Gamma_{ki}, \Gamma_{di}\}$:

$$V_1(t) = \frac{1}{2}\begin{bmatrix} s_{ip} \\ s_{ia} \end{bmatrix}^T \begin{bmatrix} H_{ipp} & H_{ipa} \\ H_{iap} & H_{iaa} \end{bmatrix}\begin{bmatrix} s_{ip} \\ s_{ia} \end{bmatrix} + \frac{1}{2}\tilde{\Omega}_i^T\Gamma_i^{-1}\tilde{\Omega}_i + \int_t^{+\infty} \varepsilon_i^2 \exp(-2\mu_i\sigma)d\sigma \tag{9}$$

where $\int_t^{+\infty} \varepsilon_i^2 \exp(-2\mu_i\sigma)d\sigma = o_i - \int_0^t \varepsilon_i^2 \exp(-2\mu_i\sigma)d\sigma$, and $o_i = \int_0^{+\infty} \varepsilon_i^2\exp(-2\mu_i\sigma)d\sigma \in (0, (\varepsilon_i^2/2\mu_i))$ is a positive constant. Then, by Property 1, (7) and $s_{ip}^T Y_{ip}\hat{\vartheta}_i = s_{ip}^T K_{ip}s_{ip}$ derived by (5), taking the derivative of (9) along (8) yield

$$\begin{aligned} \dot{V}_1(t) &= \frac{1}{2}\begin{bmatrix} s_{ip} \\ s_{ia} \end{bmatrix}^T \begin{bmatrix} \dot{H}_{ipp} & \dot{H}_{ipa} \\ \dot{H}_{iap} & \dot{H}_{iaa} \end{bmatrix}\begin{bmatrix} s_{ip} \\ s_{ia} \end{bmatrix} + \begin{bmatrix} s_{ip} \\ s_{ia} \end{bmatrix}^T \\ &\quad \times \begin{bmatrix} H_{ipp} & H_{ipa} \\ H_{iap} & H_{iaa} \end{bmatrix}\begin{bmatrix} \dot{s}_{ip} \\ \dot{s}_{ia} \end{bmatrix} - \tilde{\Omega}_i^T\begin{bmatrix} -Y_i^T s_i \\ s_{ia}^T s_{ia} \\ s_{ia} \end{bmatrix} - \zeta_i^2 \\ &= -s_{ip}^T C_{fip}s_{ip} - s_{ia}^T C_{fia}s_{ia} - s_{ip}^T Y_{ip}\vartheta_i - \tilde{K}_{ia}^T s_{ia}^T s_{ia} \\ &\quad + \tilde{\vartheta}_i^T Y_i^T s_i - s_{ia}^T(Y_{ia}\vartheta_i - D_{ia} - \tau_{ia}) - \tilde{D}_{ia}^T s_{ia} - \zeta_i^2 \\ &\leq -s_{ia}^T K_{ia}s_{ia} - \zeta_i^2 + s_{ia}^T\Big(Y_{ia}\Big(t_i^k\Big)\hat{\vartheta}_i\Big(t_i^k\Big) - Y_{ia}\hat{\vartheta}_i\Big) \\ &\quad - s_{ia}^T\Big(\hat{K}_{ia}\Big(t_i^k\Big)s_{ia}\Big(t_i^k\Big) - \hat{K}_{ia}s_{ia} + \hat{D}_{ia}\Big(t_i^k\Big) - \hat{D}_{ia}\Big) \end{aligned}$$

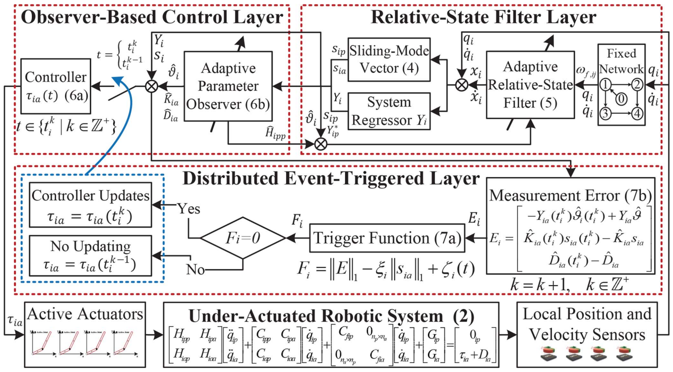

Fig. 1. Signal flow diagram of the distributed ETC algorithm over fixed communication networks.

$$
\begin{aligned}
&\le -s_{ip}^T Y_{ip}\hat{\vartheta}_i - s_{ia}^T K_{ia} s_{ia} - s_{ia}^T\big(1_3^T \otimes 1_{n_a}\big)E_i - \zeta_i^2\\
&\le -\lambda_{\min}(K_{ia})\|s_{ia}\|_1^2 + \|s_{ia}\|_1\|E_i\|_1 - \zeta_i^2\\
&\le (\xi_i - \lambda_{\min}(K_{ia}))\|s_{ia}\|_1^2 - \zeta_i\|s_{ia}\|_1 - \zeta_i^2\\
&\le \frac{1}{4}(4\xi_i - 4\lambda_{\min}(K_{ia}) + 1)\|s_{ia}\|_1^2 - \frac{1}{4}(\|s_{ia}\|_1 + 2\zeta_i)^2
\end{aligned}
$$

where if $\lambda_{\min}(K_{ia}) \ge 1/4 + \xi_i$, it gives $\dot{V}_1(t) \le 0$ and reveals $V_1(t) \in \mathbb{L}_\infty$, that is, $s_i = [s_{ip}^T, s_{ia}^T]^T \in \mathbb{L}_\infty$ and $\tilde{\Omega}_i \in \mathbb{L}_\infty$. Then, it gives $\dot{s}_i = [\dot{s}_{ip}^T, \dot{s}_{ia}^T]^T \in \mathbb{L}_\infty$ by (8). Thus, it can be concluded that $s_i(\infty) \to 0$ by Lemma 1.

Design $s_a = [s_{1a}^T, \ldots, s_{Na}^T]^T$, $\alpha = \mathrm{diag}\{\alpha_1, \ldots, \alpha_N\}$, and $\Delta_1 = q_a - (1_N \otimes q_{0a})$ with $q_a = [q_{1a}^T, \ldots, q_{Na}^T]^T$, and combining with (4) and (5) yields

$$\dot{\Delta}_1 = -\big(\alpha\mathcal{W} \otimes I_{n_a}\big)\Delta_1 + s_a. \tag{10}$$

Note that $\mathcal{W}$ has positive real parts by Lemma 2, such that (10) is input-to-state stable with $\Delta_1(\infty) \to 0$, that is, $q_{ija}(\infty) = 0$ $\forall i, j \in \mathcal{V}$, by Lemma 3, and thus $\dot{\Delta}_1(\infty) \to 0$, that is, $\dot{q}_a(\infty) \to 0$. By dynamics (2), one obtains $\ddot{q}_{ip} = -H_{ipp}^{-1}(C_{ipp} + C_{fip})\dot{q}_{ip} - H_{ipp}^{-1}(H_{ipa}\ddot{q}_{ia} + C_{ipa}\dot{q}_{ia} + G_{ip})$, then by Lemma 3 and Assumption 4, with $H_{ipp}^{-1}(H_{ipa}\ddot{q}_{ia} + C_{ipa}\dot{q}_{ia} + G_{ip}) \in \mathbb{L}_\infty$, $\dot{q}_{ip}(t_0) \in \mathbb{L}_\infty$, and $-H_{ipp}^{-1}(C_{ipp} + C_{fip})$ being Hurwitz, it can be concluded that $\dot{q}_{ip}$ is bounded. It thus follows Definition 1 that $\|(\mathcal{L}_f \otimes I_{n_a})q_a(\infty)\| \to 0$, $\|\dot{q}_a(\infty)\| \to 0$, and $\dot{q}_p(t) \in \mathbb{L}_\infty$ $\forall t \in [t_0, \infty)$.

Finally, we prove that the developed control algorithm can avoid the Zeno behavior. Define $\tilde{\Delta}_1(t) = \Delta_1(t_i^k) - \Delta_1(t)$ as $t \in [t^{k-1}, t^k)$, and it gives $\dot{\tilde{\Delta}}_1(t) = -\dot{\Delta}_1(t)$ for $\tilde{\Delta}_1(t^k) = 0$, thereby $\|\dot{\tilde{\Delta}}_1(t)\|_1 = \|\dot{\Delta}_1(t)\|_1$. By (10), it yields

$$
\begin{aligned}
\left\|\tilde{\Delta}_1(t)\right\|_1 &= \left\|\int_{t^{k-1}}^{t} \dot{\tilde{\Delta}}_1(\sigma)d\sigma\right\|_1 < \int_{t^{k-1}}^{t^k} \left\|\dot{\tilde{\Delta}}_1(\sigma)\right\|_1 d\sigma\\
&< \int_{t^{k-1}}^{t^k} \big(\lambda_{\max}(\alpha\mathcal{W})\bar{\Delta}_1 + \bar{s}_a\big)d\sigma
\end{aligned}
$$

where $\bar{\Delta}_1 = \sup_{t \ge t^{k-1}}\|\Delta_1(t)\|_1$, $\bar{s}_a = \sup_{t \ge t^{k-1}}\|s_a(t)\|$ and it implies

$$T^k = t^k - t^{k-1} > \big(Z_1\bar{\Delta}_1 + \bar{s}_a\big)^{-1}\left\|\tilde{\Delta}_1(t)\right\|_1$$

which gives $T^k > 0$, and demonstrates that the Zeno behavior can be eliminated. It thus completes the proof. ■

TABLE III
ALGORITHM II

Algorithm	The Distributed ETC Algorithm without Neighbors' Velocities
Step I	Initialize states, relative positions and observer $q_i(t_0), \dot{q}_i(t_0), x_{ip}(t_0), x_{ia}(t_0), \hat{\Omega}_i(t_0) \in \mathbb{L}_\infty$.
Step II	Obtain $x_i(t)$ and $\dot{x}_i(t)$ via the relative-position filter layer without neighbors' velocities $\dot{q}_{ja}$.
Step III	Achieve $\tau_{ia}(t)$ and $\hat{\Omega}_i(t)$ via the observer-based control layer (6) with event-triggered layer (7), then follow Step IV of Table II.

B. Distributed ETC Without Neighbors' Velocities

Notice that neighbors' velocities are usually costly to be obtained by equipping with commercially available velocity sensors and communication facilities. Thus, an enhanced distributed ETC algorithm without neighbors' velocities is then derived in Table III by designing the following distributed relative-position filter layer with only using neighbors' positions:

$$\begin{bmatrix}\dot{x}_{ip}\\ \dot{x}_{ia}\end{bmatrix} = \begin{bmatrix}\hat{H}_{ipp}^{-1}K_{ip}s_{ip} - \hat{H}_{ipp}^{-1}Y_{ip}^{*}\hat{\vartheta}_i\\ -\beta_i x_{ia} - \gamma_i \sum_{j=1}^{N}\omega_{f,ij}q_{ija} - \gamma_i b_i q_{i0a}\end{bmatrix} \tag{11}$$

where $\beta_i > 0$, $\gamma_i > 0$, and s_i, q_{ija}, q_{i0a}, and Y_{ip}^* are predefined in (4) and (5).

Theorem 2: For underactuated systems (2) with fixed communication networks, if Assumption 1 holds, the developed distributed ETC algorithm, shown in Table III, can simultaneously address the asymptotic consensus and the Zeno behavior problems, respectively, proposed in Definitions 1 and 2.

Proof: Consider a Lyapunov-like function candidate in (9), with observer-based control layer (6), event-triggered layer (7), Assumption 1, and corresponding properties, by a similar analysis, it finally gives $s_i(\infty) \to 0$ if $\lambda_{\min}(K_{ia}) \ge 1/4 + \xi_i$.

For (4) and (11), design $\beta = \mathrm{diag}\{\beta_1, \ldots, \beta_N\}$, $\gamma = \mathrm{diag}\{\gamma_1, \ldots, \gamma_N\}$, and $\Delta_2 = [q_a^T - (1_N^T \otimes q_{0a}^T), x_a^T]^T$ with $x_a = [x_{1a}^T, \ldots, x_{Na}^T]^T$, such that it can be concluded that

$$
\begin{aligned}
&\dot{\Delta}_2 = \big(\Lambda_1 \otimes I_{n_a}\big)\Delta_2 + \big(\Lambda_2 \otimes I_{n_a}\big)s_a\\
&\Lambda_1 = \begin{bmatrix}0_{N\times N} & I_N\\ -\gamma\mathcal{W} & -\beta\end{bmatrix},\ \Lambda_2 = \begin{bmatrix}I_N\\ 0_{N\times N}\end{bmatrix}.
\end{aligned} \tag{12}
$$

Note that the eigenvalues of matrix Λ_1, $\lambda(\Lambda_1) = -(1/2)\beta \pm \sqrt{(1/4)\beta^2 - \gamma W} < 0$, which means $\Delta_2 \to 0$, that is, $(\mathcal{L}_f \otimes I_{n_a})q_a(\infty)$ with input $s_a(\infty) \to 0$ under Lemma 3, such that $\dot{\Delta}_2 \to 0$, that is, $\dot{q}_a(\infty) \to 0$. Similarly, by (2), Lemma 3, and Assumption 4, it gives $\ddot{q}_{ip} = -H_{ipp}^{-1}(C_{ipp} + C_{fip})\dot{q}_{ip} - H_{ipp}^{-1}(H_{ipa}\ddot{q}_{ia} + C_{ipa}\dot{q}_{ia} + G_{ip})$, with $H_{ipp}^{-1}(H_{ipa}\ddot{q}_{ia} + C_{ipa}\dot{q}_{ia} + G_{ip}) \in \mathbb{L}_\infty$, $\dot{q}_{ip}(t_0) \in \mathbb{L}_\infty$, and $-H_{ipp}^{-1}(C_{ipp} + C_{fip})$ being Hurwitz, one obtains $\dot{q}_{ip} \in \mathbb{L}_\infty$. It thus follows (3) that $\|(\mathcal{L}_f \otimes I_{n_a})q_a(\infty)\|$, $\|\dot{q}_a(\infty)\| \to 0$, $\dot{q}_p(t) \in \mathbb{L}_\infty$ $\forall t \ge t_0$.

Then, we prove that there is no Zeno behavior. Define $\tilde{\Delta}_2(t) = \Delta_2(t_i^k) - \Delta_2(t)$ as $t \in [t_i^{k-1}, t_i^k)$, such that $\dot{\tilde{\Delta}}_2(t) = -\dot{\Delta}_2(t)$. By (12), it yields

$$\left\|\tilde{\Delta}_2(t)\right\|_1 = \left\|\int_{t^{k-1}}^{t} \dot{\Delta}_2(\sigma)d\sigma\right\|_1 < \int_{t^{k-1}}^{t^k} \|\dot{\Delta}_2(\sigma)\|_1 d\sigma$$

TABLE IV
ALGORITHM III

Algorithm	The Distributed Sampled-Data ETC Algorithm over Switched Communication Networks
Step I	Let $q_i(t_0), \dot{q}_i(t_0), \hat{q}_{ia}(t_0), x_i(t_0), \hat{\Omega}_i(t_0) \in \mathbb{L}_\infty$.
Step II	Obtain $\hat{q}_{ia}(t)$ via communication layer (14) with switched Adjacency element $\omega_{s_g,ij}$ and sampled -data estimated positions $\hat{q}_{ia}(t_i^k)$ and $\hat{q}_{ja}(t_j^{k^*})$. Obtain $x_i(t)$ and $\dot{x}_i(t)$ via filter layer (13).
Step III	Following Table II, achieve $\tau_{ia}(t)$ and $\hat{\Omega}_i(t)$ via control layer (6) with event-triggered layer (7).

$$< \left(\lambda_{\max}(\Lambda_1)\bar{\Delta}_2 + \bar{s}_a\right)\left(t^k - t^{k-1}\right)$$

where $\bar{\Delta}_2 = \sup_{t \geq t^{k-1}} \|\Delta_2(t)\|_1$ and $\bar{s}_a = \sup_{t \geq t^{k-1}} \|s_a(t)\|_1$. Therefore, we can obtain

$$T^k = t^k - t^{k-1} > \left(\lambda_{\max}(\Lambda_1)\bar{\Delta}_2 + \bar{s}_a\right)^{-1} \left\|\tilde{\Delta}_2\right\|_1 > 0$$

which eliminates the Zeno behavior, and thus finishes the proof. ■

C. Distributed Sampled-Data ETC With Switched Networks

For individuals of the system, neighbors' real positions, continuous-time communications, and fixed networks are not always available. Thus, the distributed sample-data ETC algorithm and corresponding signal flow diagram are respectively developed in Table IV and Fig. 2, by designing the following distributed relative-position filter and sampled-data communication layers

$$\dot{x}_i = \begin{bmatrix} \hat{H}_{ipp}^{-1}\left(K_{ip}s_{ip} - Y_{ip}^*\hat{\vartheta}_i\right) \\ -\varphi_i x_{ia} - \psi_i\left(q_{ia} - \hat{q}_{ia}\right) \end{bmatrix} \tag{13}$$

$$\dot{\hat{q}}_{ia} = -\eta_i \sum_{j=1}^{N} \omega_{s_g,ij}\left(\hat{q}_{ia}\left(t_i^k\right) - \hat{q}_{ja}\left(t_j^{k^*}\right)\right) \tag{14}$$

where $\varphi_i, \psi_i, \eta_i > 0$, $k^* = \arg\min_{l \in \mathbb{Z}^+ : t \geq t_j^l}\{t - t_j^l\}$, $\hat{q}_{ia}(t_i^k)$, and $\hat{q}_{ja}(t_j^{k^*})$ are sampled-data estimated positions.

Theorem 3: For underactuated systems (2) with switched networks, if Assumptions 2, 3, and the condition $\eta_i \bar{T}\lambda_{\max}(\mathcal{L}_s) \in (0, 1)$ hold, the developed distributed sampled-data ETC algorithm, shown in Table IV, can simultaneously address the asymptotic consensus and the Zeno behavior problems.

Proof: By a similar analysis performed in Theorem 1, it concludes $s_i(\infty) \to 0$. Designing $\eta = \mathrm{diag}\{\eta_1, \ldots, \eta_N\}$, $\hat{q}_a = [\hat{q}_{1a}^T, \ldots, \hat{q}_{Na}^T]^T$, and $\dot{\hat{q}}_a = [\dot{\hat{q}}_{1a}^T, \ldots, \dot{\hat{q}}_{Na}^T]^T$ for (14), it gives

$$\dot{\hat{q}}_a = -\eta\left(\mathcal{L}_{s_g} \otimes I_{n_a}\right)\hat{q}_a\left(t^k\right). \tag{15}$$

Integrating both sides of (15) along $[t^k, t^{(k+1)^-}]$, $(k+1)^- \to (k+1)$ yields

$$\hat{q}_a\left(t^{(k+1)^-}\right) = \left(\left(I_N - \eta\mathcal{L}_{s_g}T^{(k+1)^-}\right) \otimes I_{n_a}\right)\hat{q}_a\left(t^k\right).$$

By a recursive analysis, we can obtain

$$\hat{q}_a\left(t^{(k+1)^-}\right) = \prod_{g=0}^{k}\left(M_g \otimes I_{n_a}\right)\hat{q}_a\left(t^0\right) \tag{16}$$

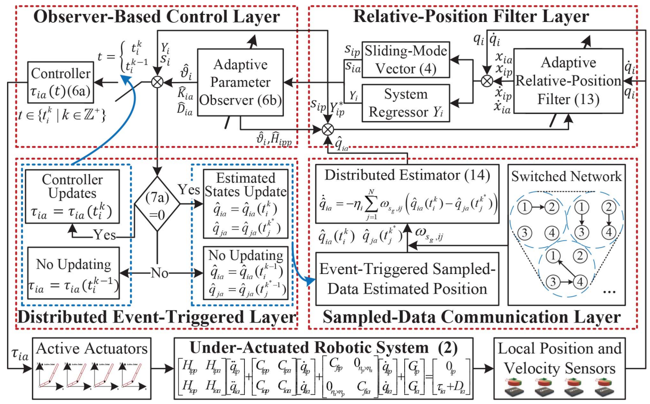

Fig. 2. Signal flow diagram of the distributed sampled-data ETC algorithm over switched communication networks.

where $\hat{q}_a(t^0) = \hat{q}_a(t_0) \in \mathbb{L}_\infty$, $k \geq g_1$ with g_1 predefined in Assumption 2, $M_g = I_N - \eta\mathcal{L}_{s_g}T^{(g+1)^-}$ is a row stochastic matrix with positive diagonal elements by Lemma 4 with $\eta_i\bar{T}\lambda_{\max}(\mathcal{L}_{s_g}) \in (0, 1)$ and $M_g 1_N = 1_N$. Then, by Lemma 5, it gives

$$\prod_{g=0}^{k} M_g \geq \hbar \sum_{g=0}^{k} M_g \tag{17}$$

where $\sum_{g=0}^{k} \eta\mathcal{L}_{s_g}T^{(g+1)^-}$ has only one eigenvalue as 0 by Assumption 2 with $\eta, T^{(g+1)^-} > 0$. Then, with the fact $\sum_{g=0}^{k} M_g 1_N = (k+1)1_N$, it gives that the eigenvalue $k+1$ of $\sum_{g=0}^{k} M_g$ is of algebraic multiplicity 1, such that $\mathcal{G}(\sum_{g=0}^{k} M_g)$ contains a spanning tree by Lemma 6. Then, it follows that $\mathcal{G}(\prod_{g=0}^{k} M_g)$ contains a spanning tree by (17). Combining with that $\prod_{g=0}^{k} M_g$ is a row stochastic matrix with positive diagonal elements, we can obtain that $\prod_{g=0}^{k} M_g$ is SIA by Lemma 7. Thus, it can be concluded that $\prod_{g=0}^{k} M_g = 1_N y^T$ for a constant column vector $y \in \mathbb{R}^N$ by Lemma 8. It thus follows (16) that

$$\lim_{t\to\infty} \hat{q}_a(t) = \lim_{k\to\infty} \hat{q}_a\left(t^{(k+1)^-}\right) = \left(1_N y^T \otimes I_{n_a}\right)\hat{q}_a\left(t^0\right) \tag{18}$$

which means $\hat{q}_a(\infty) \in \mathbb{L}_\infty$, $\dot{\hat{q}}_a(\infty) \to 0$, and $\hat{q}_{ia}(\infty) = \hat{q}_{ja}(\infty)$ for $i, j \in \mathcal{V}$.

For (4) and (13), design $\varphi = \mathrm{diag}\{\varphi_1, \ldots, \varphi_N\}$, $\psi = \mathrm{diag}\{\psi_1, \ldots, \psi_N\}$, and $\Delta_3 = [\tilde{q}_a^T, x_a^T]^T$ with $\tilde{q}_a = [\tilde{q}_{1a}^T, \ldots, \tilde{q}_{Na}^T]^T$ and $\tilde{q}_a = q_a - \hat{q}_a$, then one obtains

$$\dot{\Delta}_3 = \left(\Lambda_3 \otimes I_{n_a}\right)\Delta_3 + \left(\Lambda_2 \otimes I_{n_a}\right)\left(s_a - \dot{\hat{q}}_a\right)$$

$$\Lambda_3 = \begin{bmatrix} 0_{N\times N} & I_N \\ -\psi & -\varphi \end{bmatrix}, \quad \Lambda_2 = \begin{bmatrix} I_N \\ 0_{N\times N} \end{bmatrix}.$$

Note that the eigenvalues of matrix Λ_3 $\lambda(\Lambda_3) = -(1/2)\varphi \pm \sqrt{(1/4)\varphi^2 - \psi} < 0$, which means $\Delta_3 \to 0$, that is, $q_a(\infty) - \hat{q}_a(\infty) \to 0$ with input $s_a(\infty) - \dot{\hat{q}}_a(\infty) \to 0$ under Lemma 3, such that $\dot{\Delta}_3 \to 0$, that is, $\dot{q}_a(\infty) - \dot{\hat{q}}_a(\infty) \to 0$. Combining with $\hat{q}_{ia}(\infty) = \hat{q}_{ja}(\infty)$ and $\dot{\hat{q}}_a(\infty) \to 0$, we can obtain $\|(\mathcal{L}_{s_g} \otimes I_{n_a})q_a(\infty)\|$, $\|\dot{q}_a(\infty)\| \to 0$ in Definition 1. Similarly, it gives $\ddot{q}_{ip} = -H_{ipp}^{-1}(C_{ipp} + C_{fip})\dot{q}_{ip} - H_{ipp}^{-1}(H_{ipa}\ddot{q}_{ia} + C_{ipa}\dot{q}_{ia} + G_{ip})$ with Lemma 3 and Assumption 4, such that $\dot{q}_p(t) \in \mathbb{L}_\infty$.

Meanwhile, the Zeno behavior can also be eliminated by a similar analysis, and the proof is completed. ■

D. Further Results and Discussion

Note that the distributed sampled-data ETC algorithm in Table IV can be further extended to centralized sampled-data ETC algorithm with the following centralized event-triggered and communication layers

$$\begin{cases} F = \|E\|_1 - \xi\|s_a\|_1 - \varepsilon\exp(-\mu t) & \text{(19a)} \\ E = \begin{bmatrix} -Y_a(t^k)\hat{\vartheta}(t^k) + Y_a\hat{\vartheta} \\ \hat{K}_a(t^k)s_a(t^k) - \hat{K}_a s_a \\ \hat{D}_a(t^k) - \hat{D}_a \end{bmatrix} & \text{(19b)} \end{cases}$$

$$\dot{\hat{q}}_{ia} = -\eta\sum_{j=1}^{N}\omega_{s_g,ij}\left(\hat{q}_{ia}\left(t^k\right) - \hat{q}_{ja}\left(t^k\right)\right) \tag{20}$$

where ξ, ε, μ, and η are positive constants, with $\mu \in (0, 1)$ and $\eta \in (0, 1/\bar{T}\lambda_{\max}(\mathcal{L}_{s_g}))$.

Corollary 1: For underactuated systems (2) with the switched network, if Assumptions 2 and 3 hold, the centralized sampled-data ETC algorithm, with centralized event-triggered layer (19) and centralized communication layer (20), can address the asymptotic consensus and Zeno behavior problems.

In addition, the control algorithm in Table IV can be extended to a distributed sampled-data time-triggered control algorithm by designing the following distributed time-triggered and communication layers, with asynchronously fixed trigger time interval $T_i \in (0, 1/\eta_i\lambda_{\max}(\mathcal{L}_{s_g}))$

$$F_i = -\mathrm{mod}(t, T_i),\ \ i \in \mathcal{V} = \{1, \ldots, N\} \tag{21a}$$

$$\dot{\hat{q}}_{ia} = -\eta_i\sum_{j=1}^{N}\omega_{s_g,ij}\left(\hat{q}_{ia}\left(t_i^k\right) - \hat{q}_{ja}\left(t_j^{k^*}\right)\right). \tag{21b}$$

Corollary 2: For underactuated systems (2) with the switched network, if Assumption 2 holds, the distributed sampled-data time-triggered control algorithm, with distributed time-triggered and sampled-data communication layers (21), can address the asymptotic consensus and Zeno behavior problems.

Finally, the control algorithm in Table IV can be extended to a centralized sampled-data time-triggered control algorithm by designing the following centralized time-triggered and communication layers, with synchronously fixed trigger time interval $T \in (0, 1/\eta\lambda_{\max}(\mathcal{L}_{s_g}))$

$$F = -\mathrm{mod}(t, T) \tag{22a}$$

$$\dot{\hat{q}}_{ia} = -\eta\sum_{j=1}^{N}\omega_{s_g,ij}\left(\hat{q}_{ia}\left(t^k\right) - \hat{q}_{ja}(t^k)\right). \tag{22b}$$

Corollary 3: For underactuated systems (2) with a switched network, if Assumption 2 holds, the centralized sampled-data time-triggered control algorithm, with centralized time-triggered and communication layers (22), can address the asymptotic consensus and Zeno behavior problems.

Proof: The proofs of Corollaries 1–3 are similar to that of Theorem 3 and thus are omitted. ■

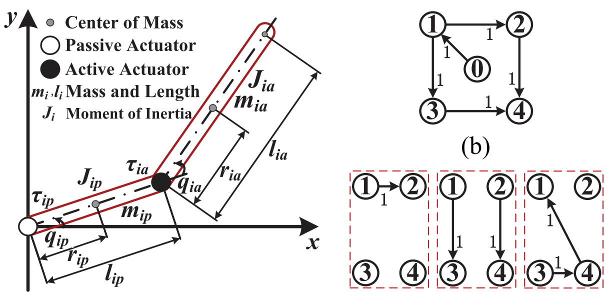

Fig. 3. (a) Two-actuator planar manipulator. (b) Fixed communication network with a static leader. (c) Switched communication network with switching subnetworks.

Remark 5: In contrast to the control of underactuated systems over fixed communication networks [10]–[12], this article comprehensively investigates it by developing numerous novel ETC algorithms over both fixed and switched networks, where the analysis with discrete-time communications and switched interconnections among individuals are much more challenging. Specifically, the developed control algorithms are insensitive to internal uncertainties and external disturbances, which extends the special cases in [35]–[38].

Remark 6: The obtained algorithms take into account more challenges, for instance, as opposed to ETC methods in [28]–[32] with continuous-time communications, this article presents sampled-data communication rules driven by ETC and time-triggered mechanisms, which can reduce the energy cost and thereby relax the requirement of wide communication bandwidth. In comparison with some results relying on neighbors' velocities or real positions [34], [39], [40], this article can achieve the control objective by only using neighbors' estimated positions, which removes the impractical assumptions and thereby further save the control resources.

Remark 7: One of the main motivations is to save the control cost, including the controller updating cost and communication cost. For the controller updating cost, a proper ETC mechanism plays the most important role in determining the updating frequency of controllers, which can be described by the trigger numbers shown in the hereinafter simulations. While the communication cost among individuals is generally decided by the number of transmission states and length of the transmission interval, and the sampled-data communication with neighbors' partial states can reduce this cost.

IV. Simulation

Based on the structure, communication networks, physical and control parameters of four two-actuator planar manipulators, respectively, displayed in Fig. 3 and Table V [42], as well as the four-order Runge–Kutta simulation environment with total computation numbers of each control input as 10 000, three examples are performed for the developed control algorithms in Theorems 1–3 and Corollaries 1–3.

Example 1: Based on the fixed communication network shown in Fig. 3(b), the example results of Theorems 1 and 2 are displayed in Figs. 4 and 5. Fig. 4 depicts the trajectories of active and passive actuators, where the positions and

TABLE V
PHYSICAL AND CONTROL PARAMETERS

Physical parameters	$m_i = [2, 2]$, $l_i = [1.5, 1.5]$, $r_i = [0.75, 0.75]$ $J_i = [1.5, 1.5]$, $H_{ipp} = \vartheta_{i1} + 2\vartheta_{i2}\cos q_{ia}$ $H_{ipa} = H_{iap} = \vartheta_{i3} + \vartheta_{i2}\cos q_{ia}$, $H_{iaa} = \vartheta_{i3}$ $C_{ipp} = -\vartheta_{i2}\dot{q}_{ia}\sin q_{ia}$, $C_{iap} = \vartheta_{i2}\dot{q}_{ip}\sin q_{ia}$ $C_{ipa} = -\vartheta_{i2}(\dot{q}_{ip} + \dot{q}_{ia})\sin q_{ia}$, $C_{iaa} = 0$ $C_{fip} = \|C_{ipp}\|_2 + 1$, $C_{fia} = \|C_{iaa}\|_2 + 1$ $G_{ip} = 9.8\vartheta_{i4}\cos q_{ip} + 9.8\vartheta_{i5}\cos(q_{ip} + q_{ia})$ $G_{ia} = 9.8\vartheta_{i5}\cos(q_{ip} + q_{ia})$, $D_{ia} = 0.5$ $\vartheta_{i1} = m_{ip}r_{ip}^2 + m_{ia}(l_{ip}^2 + r_{ia}^2) + J_{ip} + J_{ia}$ $\vartheta_{i2} = m_{ia}l_{ip}r_{ia}$, $\vartheta_{i3} = m_{ia}r_{ia}^2 + J_{ia}$ $\vartheta_{i4} = m_{ip}r_{ip} + m_{ia}l_{ip}$, $\vartheta_{i5} = m_{ia}l_{ia}$ $q_i(0) = [i - 2.5, i - 2.5]^T$, $\dot{q}_i(0) = -q_i(0)$, $\hat{\vartheta}_i(0) = [8.75, 1.25, 1.38, 3.5, 2]^T$, $i \in \{1, 2, 3, 4\}$
Control parameters	$\alpha_i = 1.5$, $\beta = \varphi_i = 4$, $\gamma_i = \psi_i = \eta_i = 6$, $\xi_i = 1$ $\varepsilon_i = 2$, $\mu_i = 0.2$, $K_{ip} = 15$, $\Gamma_{ki} = 15$, $\Gamma_{di} = 5$ $\Gamma_{\vartheta i} = 0.8I_5$, $x_{ip}(0) = 0$, $x_{ia}(0) = 0$, $\hat{q}_{ia}(0) = 0$ $q_{0a} = 0$, $\hat{K}_{ia}(0) = 0$, $\hat{D}_{ia}(0) = 0$, $i \in \{1, 2, 3, 4\}$

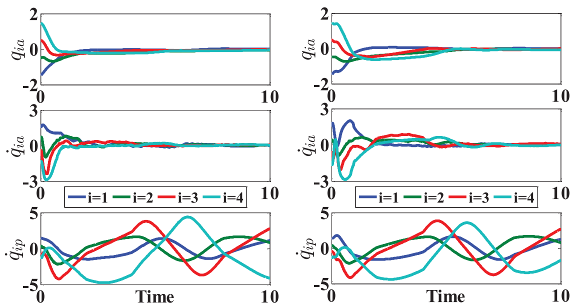

(a) (b)

Fig. 4. Convergence trajectories of q_{ia} and $\dot{q}_{ia}$ and bounded trajectories of $\dot{q}_{ip}$ in (a) Theorem 1 and (b) Theorem 2.

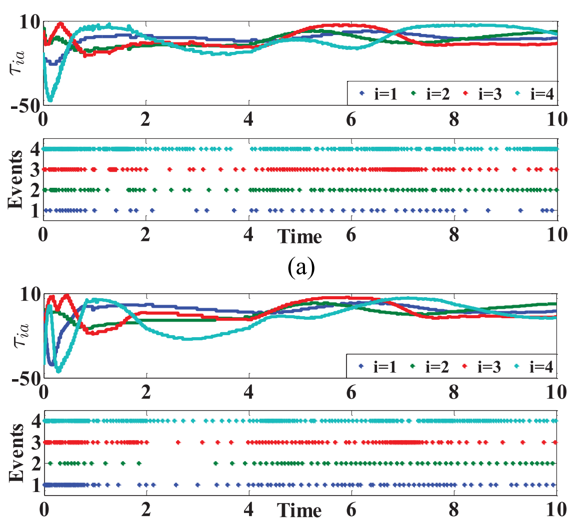

(b)

Fig. 5. Control inputs and trigger numbers of (a) Theorem 1 and (b) Theorem 2.

velocities of active actuators reach to 0, and the velocities of passive actuators are bounded by $[-5, 5]$. Fig. 5 depicts the control inputs and trigger numbers, where the trigger numbers in Theorem 1 are 51, 104, 263, and 516, and those in Theorem 2 are 108, 68, 117, and 204.

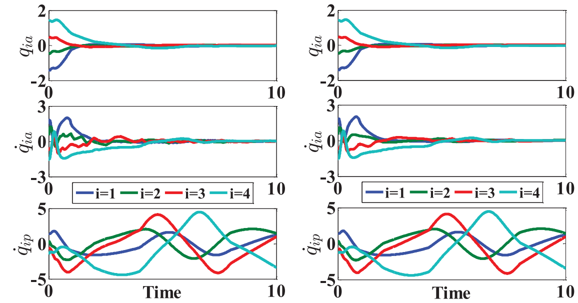

(a) (b)

Fig. 6. Convergence trajectories of q_{ia} and $\dot{q}_{ia}$ and bounded trajectories of $\dot{q}_{ip}$ in (a) Theorem 3 and (b) Corollary 1.

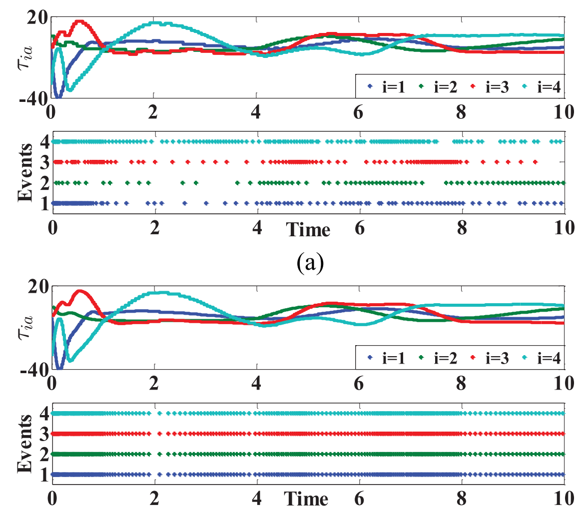

(b)

Fig. 7. Control inputs and trigger numbers of (a) Theorem 3 and (b) Corollary 1.

Example 2: Based on the switched communication network shown in Fig. 3(c), the example results of Theorem 3 and Corollary 1 are displayed in Figs. 6 and 7. Fig. 6 depicts that the positions and velocities of active actuators, respectively, reach to the same state and 0, and the velocities of passive actuators are bounded by $[-5, 5]$. Fig. 7 depicts that the trigger numbers in Theorem 3 are 108, 73, 96, and 153, and those in Corollary 1 are 206, 206, 206, and 206.

Example 3: Based on the same switched communication network, the example results of Corollaries 2 and 3 are displayed in Figs. 8 and 9. By Fig. 8, we conclude that the positions and velocities of active actuators, respectively, reach to the same state and 0, and the velocities of passive actuators are bounded by $[-5, 5]$. By Fig. 9, we obtain the trigger numbers in Corollary 2 are 523, 463, 422, and 400, and those in Corollary 3 are 463, 463, 463, and 463.

Average Trigger Rate: The performance comparison is enumerated in Fig. 10, which clearly reveals that: 1) the control cost of distributed algorithms are less than that of centralized algorithms; 2) the ETC algorithms are more efficient than the time-triggered algorithms; and 3) it requires the

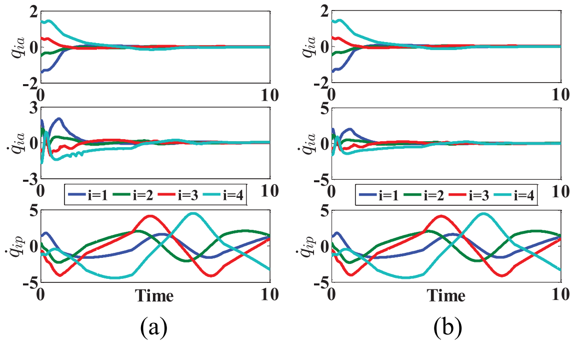

Fig. 8. Convergence trajectories of q_{ia} and $\dot{q}_{ia}$ and bounded trajectories of $\dot{q}_{ip}$ in (a) Corollary 2 and (b) Corollary 3.

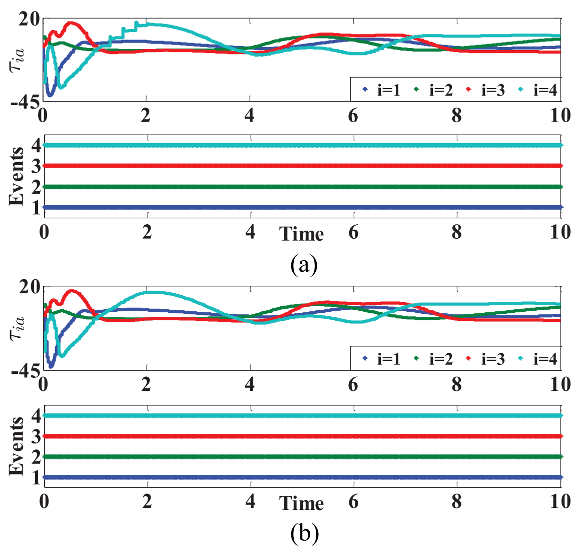

Fig. 9. Control inputs and trigger numbers of (a) Corollary 2 and (b) Corollary 3.

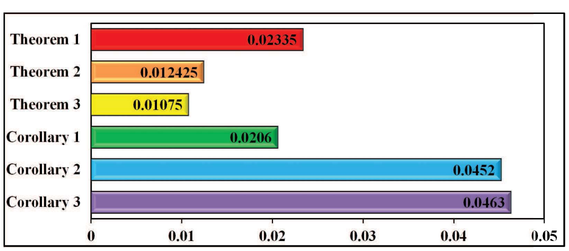

Fig. 10. Average trigger rates of theorems and corollaries.

least control resources for the distributed sampled-data ETC algorithm.

Remark 8: Note that the obtained results cover some existing methods and some of them can be seen as the comparison examples. First, Theorem 1 covers the ETC algorithms with continuous-time communications and neighbors' velocities. Second, Corollary 1 covers the centralized ETC cases. Third, Corollaries 2 and 3 cover the time-triggered cases. In conclusion, the developed algorithms provide more solutions for the theoretical and practical research of underactuated systems.

V. Conclusion

This article has investigated the consensus problem of a networked underactuated robotic system with internal uncertainties and external disturbances. First, a distributed ETC algorithm over a fixed communication network has been developed to provide satisfactory control performances with fewer control costs. Second, an ETC algorithm with a relative-position filter layer has been designed without using the neighbors' velocities. Third, a sampled-data ETC algorithm with a distributed sampled-data estimator layer has been designed over switched communication networks, which can further reduce unnecessary control cost without requiring the neighbors' real positions. It has been proved that the developed ETC algorithms can simultaneously guarantee the convergence of the active states and the boundedness of the velocities of passive actuators without Zeno behaviors. Finally, three other sampled-data control algorithms with performance comparisons are presented by extending the developed results to different cases. Future works will be focused on the sampled-data ETC of underactuated systems with the Markovian chains and the convergence of passive states.

References

[1] Z. Meng, T. Yang, G. Shi, D. V. Dimarogonas, Y. Hong, and K. H. Johansson, "Targeted agreement of multiple Lagrangian systems," *Automatica*, vol. 84, pp. 109–116, Oct. 2017.

[2] Z. Liu, G. Wen, X. Yu, Z. Guan, and T. Huang, "Delayed impulsive control for consensus of multiagent systems with switching communication graphs," *IEEE Trans. Cybern.*, vol. 50, no. 7, pp. 3045–3055, Jul. 2020.

[3] K. Li, C. Hua, X. You, and X. Guan, "Distributed output-feedback consensus control for nonlinear multiagent systems subject to unknown input delays," *IEEE Trans. Cybern.*, early access, Jun. 3, 2020, doi: 10.1109/TCYB.2020.2993297.

[4] X. Wang, G. Wang, and S. Li, "Distributed finite-time optimization for disturbed second-order multiagent systems," *IEEE Trans. Cybern.*, early access, May 21, 2020, doi: 10.1109/TCYB.2020.2988490.

[5] C. L. P. Chen, G. Wen, Y. Liu, and Z. Liu, "Observer-based adaptive backstepping consensus tracking control for high-order nonlinear semi-strict-feedback multiagent systems," *IEEE Trans. Cybern.*, vol. 46, no. 7, pp. 1591–1601, Jul. 2016.

[6] X. Chang and G. Yang, "Nonfragile H_∞ filtering of continuous-time fuzzy systems," *IEEE Trans. Signal Process.*, vol. 59, no. 4, pp. 1528–1538, Apr. 2011.

[7] M. Ge, Z. Guan, B. Hu, D. He, and R. Liao, "Distributed controller–estimator for target tracking of networked robotic systems under sampled interaction," *Automatica*, vol. 69, pp. 410–417, Jul. 2016.

[8] X. Xie and X. Mu, "Observer-based intermittent consensus control of nonlinear singular multi-agent systems," *Int. J. Control, Autom. Syst.*, vol. 17, pp. 2321–2330, Jul. 2019.

[9] X. Guo, J. Liang, and J. Lu, "Finite-time asymmetric bipartite consensus for signed networks of dynamic agents," *Int. J. Control, Autom. Syst.*, vol. 17, pp. 1041–1049, Mar. 2019,

[10] J. Huang, S. Ri, T. Fukuda, and Y. Wang, "A disturbance observer based sliding mode control for a class of underactuated robotic system with mismatched uncertainties," *IEEE Trans. Autom. Control*, vol. 64, no. 6, pp. 2480–2487, Jun. 2019.

[11] T. Chen and J. Shan, "Distributed tracking of a class of underactuated Lagrangian systems with uncertain parameters and actuator faults," *IEEE Trans. Ind. Electron.*, vol. 67, no. 5, pp. 4244–4253, May 2020.

[12] D. Pucci, F. Romano, and F. Nori, "Collocated adaptive control of underactuated mechanical systems," *IEEE Trans. Robot.*, vol. 31, no. 6, pp. 1527–1536, Dec. 2015.

[13] B. Lu, Y. Fang, and N. Sun, "Continuous sliding mode control strategy for a class of nonlinear underactuated systems," *IEEE Trans. Autom. Control*, vol. 63, no. 10, pp. 3471–3478, Oct. 2018.

[14] J. Huang, Z. Guan, T. Matsuno, T. Fukuda, and K. Sekiyama, "Sliding-mode velocity control of mobile-wheeled inverted-pendulum systems," *IEEE Trans. Robot.*, vol. 26, no. 4, pp. 750–758, Aug. 2010.

[15] J. Huang, M. Zhang, S. Ri, C. Xiong, Z. Li, and Y. Kang, "High-order disturbance-observer-based sliding mode control for mobile wheeled inverted pendulum systems," *IEEE Trans. Ind. Electron.*, vol. 67, no. 3, pp. 2030–2041, Mar. 2020.

[16] J. H. Park, H. Shen, X. Chang, and T. H. Lee, *Recent Advances in Control and Filtering of Dynamic Systems With Constrained Signals*. Cham, Switzerland: Springer, 2018. doi: 10.1007/978-3-319-96202-3.

[17] M. Ajina, D. Tabatabai, and C. Nowzari, "Asynchronous distributed event-triggered coordination for multiagent coverage control," *IEEE Trans. Cybern.*, early access, Jan. 23, 2020, doi: 10.1109/TCYB.2019.2962772.

[18] Z. Gu, P. Shi, D. Yue, and Z. Ding, "Decentralized adaptive event-triggered H_∞ filtering for a class of networked nonlinear interconnected systems," *IEEE Trans. Cybern.*, vol. 49, no. 5, pp. 1570–1579, May 2019.

[19] Y. Li, L. Liu, C. Hua, and G. Feng, "Event-triggered/self-triggered leader-following control of stochastic nonlinear multiagent systems using high-gain method," *IEEE Trans. Cybern.*, early access, Sep. 4, 2019, doi: 10.1109/TCYB.2019.2936413.

[20] H. Zhang, J. H. Park, D. Yue, and C. Dou, "Data-driven optimal event-triggered consensus control for unknown nonlinear multi-agent systems with control constraints," *Int. J. Robust Nonlinear Control*, vol. 29, pp. 4828–4844, Sep. 2019.

[21] X. Yao, H. Ding, M. Ge, and J. H. Park, "Event-triggered synchronization control of networked Euler–Lagrange systems without requiring relative velocity information," *Inf. Sci.*, vol. 508, pp. 183–199, Jan. 2020.

[22] J. Cheng, C. K. Ahn, H. R. Karimi, J. Cao, and W. Qi, "An event-based asynchronous approach to Markov jump systems with hidden mode detections and missing measurements," *IEEE Trans. Syst., Man, Cybern., Syst.*, vol. 49, no. 9, pp. 1749–1758, Sep. 2019.

[23] H. Shen, F. Li, H. Yan, H. R. Karimi, and H.-K. Lam, "Finite-time event-triggered $\mathcal{H}_\infty$ control for T–S fuzzy Markov jump systems," *IEEE Trans. Fuzzy Syst.*, vol. 26, no. 5, pp. 3122–3135, Oct. 2018.

[24] Y. Liu, B. Guo, J. H. Park, and S. Lee, "Event-based reliable dissipative filtering for T–S fuzzy systems with asynchronous constraints," *IEEE Trans. Fuzzy Syst.*, vol. 26, no. 4, pp. 2089–2098, Aug. 2018.

[25] B. Hu, Z. Guan, and M. Fu, "Distributed event-driven control for finite-time consensus," *Automatica*, vol. 103, pp. 88–95, May 2019.

[26] S. Yan, S. K. Nguang, M. Shen, and G. Zhang, "Event-triggered $\mathcal{H}_\infty$ control of networked control systems with distributed transmission delay," *IEEE Trans. Autom. Control*, vol. 65, no. 10, pp. 4295–4301, Oct. 2020, doi: 10.1109/TAC.2019.2953460.

[27] C. Wang, C. Wen, and Q. Hu, "Event-triggered adaptive control for a class of nonlinear systems with unknown control direction and sensor faults," *IEEE Trans. Autom. Control*, vol. 65, no. 2, pp. 763–770, Feb. 2020, doi: 10.1109/TAC.2019.2916999.

[28] R. Postoyan, M. C. Bragagnolo, E. Galbrun, J. Daafouz, D. Nešić, and E. B. Casteland, "Event-triggered tracking control of unicycle mobile robots," *Automatica*, vol. 52, pp. 302–308, Feb. 2015.

[29] N. Xu, Y. Chen, A. Xue, G. Zong, and X. Zhao, "Event-trigger-based adaptive fuzzy hierarchical sliding mode control of uncertain under-actuated switched nonlinear systems," *ISA Trans.*, to be published, doi: 10.1016/j.isatra.2019.11.011.

[30] C. Liu, J. Gao, G. J. Zhang, and D. Xu, "Robust event-triggered model predictive control for straight-line trajectory tracking of underactuated underwater vehicles," in *Proc. OCEANS*, Aberdeen, U.K., 2017, pp. 1–5, doi: 10.1109/OCEANSE.2017.8084632.

[31] S. J. Yoo and B. S. Park, "Guaranteed-connectivity-based distributed robust event-triggered tracking of multiple underactuated surface vessels with uncertain nonlinear dynamics," *Nonlinear Dyn.*, vol. 99, pp. 2233–2249, Jan. 2020.

[32] M. Li, T. Li, X. Gao, Q. Shan, C. L. P. Chen, and Y. Xiao, "Adaptive NN event-triggered control for path following of underactuated vessels with finite-time convergence," *Neurocomputing*, vol. 379, pp. 203–213, Feb. 2020.

[33] X. You, C. Hua, and X. Guan, "Event-triggered leader-following consensus for nonlinear multiagent systems subject to actuator saturation using dynamic output feedback method," *IEEE Trans. Autom. Control*, vol. 63, no. 12, pp. 4391–4396, Dec. 2018.

[34] J. Yang, J. Sun, W. Zheng, and S. Li, "Periodic event-triggered robust output feedback control for nonlinear uncertain systems with time-varying disturbance," *Automatica*, vol. 94, pp. 324–333, Aug. 2018.

[35] H. Li, X. Liao, T. Huang, and W. Zhu, "Event-triggering sampling based leader-following consensus in second-order multi-agent systems," *IEEE Trans. Autom. Control*, vol. 60, no. 7, pp. 1998–2003, Jul. 2015.

[36] H. Li, G. Chen, T. Huang, Z. Dong, W. Zhu, and L. Gao, "Event-triggered distributed average consensus over directed digital networks with limited communication bandwidth," *IEEE Trans. Cybern.*, vol. 46, no. 12, pp. 3098–3110, Dec. 2016.

[37] J. Cheng, J. H. Park, L. Zhang, and Y. Zhu, "An asynchronous operation approach to event-triggered control for fuzzy Markovian jump systems with general switching policies," *IEEE Trans. Fuzzy Syst.*, vol. 26, no. 1, pp. 6–18, Feb. 2018.

[38] Z. Wu, Y. Xu, R. Lu, Y. Wu, and T. Huang, "Event-triggered control for consensus of multiagent systems with fixed/switching topologies," *IEEE Trans. Syst., Man, Cybern., Syst.*, vol. 48, no. 10, pp. 1736–1746, Oct. 2018.

[39] X. Chu, Z. Peng, G. Wen, and A. Rahmani, "Distributed formation tracking of nonholonomic autonomous vehicles via event-triggered and sampled-data method," *Int. J. Control*, vol. 92, no. 10, pp. 2243–2254, Oct. 2019.

[40] Y. Deng, X. Zhang, N. Im, G. Zhang, and Q. Zhang, "Model-based event-triggered tracking control of underactuated surface vessels with minimum learning parameters," *IEEE Trans. Neural Netw. Learn. Syst.*, early access, Nov. 25, 2019, doi: 10.1109/TNNLS.2019.2951709.

[41] J. Yang, F. Xiao, and T. Chen, "Event-triggered formation tracking control of nonholonomic mobile robots without velocity measurements," *Automatica*, vol. 112, no. 10, Feb. 2020, Art. no. 108671.

[42] M. W. Spong, S. Hutchinson, and M. Vidyasagar, *Robot Modeling and Control*. New York, NY, USA: Wiley, 2006.

[43] H. K. Khalil and J. W. Grizzle, *Nonlinear Systems*. Upper Saddle River, NJ, USA: Prentice-Hall, 1996.

[44] J. Mei, W. Ren, and G. Ma, "Distributed containment control for Lagrangian networks with parametric uncertainties under a directed graph," *Automatica*, vol. 48, no. 4, pp. 653–659, Apr. 2012.

[45] E. D. Sontag, "Input to state stability: Basic concepts and results," in *Nonlinear and Optimal Control Theory*. Cham, Switzerland: Springer, pp. 163–220, 2008.

[46] M. Ge, Z. Liu, G. Wen, X. Yu, and T. Huang, "Hierarchical controller-estimator for coordination of networked Euler–Lagrange systems," *IEEE Trans. Cybern.*, vol. 50, no. 6, pp. 2450–2461, Jun. 2020.

[47] A. Jadbabaie, J. Lin, and A. S. Morse, "Coordination of groups of mobile autonomous agents using nearest neighbor rules," *IEEE Trans. Autom. Control*, vol. 48, no. 6, pp. 988–1001, Jun. 2003.

[48] W. Ren and R. W. Beard, "Consensus seeking in multiagent systems under dynamically changing interaction topologies," *IEEE Trans. Autom. Control*, vol. 50, no. 5, pp. 655–661, May 2005.

[49] Z. Liu, Z. Guan, X. Shen, and G. Feng, "Consensus of multi-agent networks with aperiodic sampled communication via impulsive algorithms using position-only measurements," *IEEE Trans. Autom. Control*, vol. 57, no. 10, pp. 2639–2643, Oct. 2012.

[50] J. Wolfowitz, "Products of indecomposable, aperiodic, stochastic matrices," *Proc. Amer. Math. Soc. USA*, vol. 14, no. 5, pp. 733–736, 1963.

Xiang-Yu Yao received the B.S. degree from the China University of Geosciences, Wuhan, China, in 2015, where he is currently pursuing the Ph.D. degree with the School of Mechanical Engineering and Electronic Information.

From 2019 to 2020, he is a Visiting Scholar with the Department of Electrical Engineering, Yeungnam University, Gyeongsan, South Korea. His current research interests include event-triggered control, fault-tolerant control, and sampled-data control of networked systems.

Ju H. Park (Senior Member, IEEE) received the Ph.D. degree in electronics and electrical engineering from the Pohang University of Science and Technology (POSTECH), Pohang, South Korea, in 1997.

From 1997 to 2000, he was a Research Associate with the Engineering Research Center-Automation Research Center, POSTECH. He joined Yeungnam University, Gyeongsan, South Korea, in 2000, where he is currently the Chuma Chair Professor. He has published a number of papers in these areas. He has co-authored the monographs: *Recent Advances in Control and Filtering of Dynamic Systems With Constrained Signals* (New York, NY, USA: Springer/Nature, 2018) and *Dynamic Systems With Time Delays: Stability and Control* (New York, NY, USA: Springer/Nature, 2019). His research interests include robust control and filtering, neural/complex networks, fuzzy systems, multiagent systems, and chaotic systems.

Prof. Park is a recipient of the Highly Cited Researcher Award by Clarivate Analytics (formerly, Thomson Reuters), since 2015 and was listed in three fields: engineering, computer sciences, and mathematics in 2019. He serves as an Editor of *International Journal of Control, Automation and Systems* and an edited volume: *Recent Advances in Control Problems of Dynamical Systems and Networks* (New York, NY, USA: Springer/Nature, 2020). He is also a Subject Editor/Advisory Editor/Associate Editor/Editorial Board Member for several international journals, including *IET Control Theory and Applications*, *Applied Mathematics and Computation*, *Journal of the Franklin Institute*, *Nonlinear Dynamics*, *Engineering Reports*, *Cogent Engineering*, IEEE TRANSACTIONS ON FUZZY SYSTEMS, IEEE TRANSACTIONS ON NEURAL NETWORKS AND LEARNING SYSTEMS, IEEE TRANSACTIONS ON CYBERNETICS, and so on. He is a Fellow of the Korean Academy of Science and Technology.

Hua-Feng Ding received the B.S., M.S., and first Ph.D. degrees in mechanical engineering from Yanshan University, Qinghuadao, China, in 2000, 2003, and 2007, respectively, and the second Ph.D. degree in mechanical engineering from the University of Duisburg–Essen, Essen, Germany, in 2015.

He was an Associate Professor with Yanshan University, from 2007 to 2011, and became a Professor and a Ph.D. Supervisor from 2011 to 2014. He was an Alexander von Humboldt Research Fellow with the University of Duisburg–Essen from 2010 to 2012. He is currently a Professor and a Ph.D. Supervisor with the China University of Geosciences, Wuhan, China, where he is also the President of the School of Mechanical Engineering and Electronic Information. He has coauthored four books and published over 100 refereed journal papers. He holds 32 patents. His research and teaching interests include mechatronics, digital prototyping, innovative design, and control of mechanical equipment.

Prof. Ding was a recipient of the one-hundred outstanding innovative talents, Hebei, in 2010, and the National Hundred Excellent Doctoral Dissertation Nomination Thesis Award, German, the Humboldt Scholar, Hebei, in 2011, the 333 Talent Project Second-Level Talent in 2013, and the Fok Ying-Tong Education Fund, and the National Outstanding Youth Fund in 2014. He was the Vice President of the Wuhan Mechanical Engineering Society, the Session Chair of the 2015 ASME Conference, the Director of the Chinese Society of Mechanical Engineering, the Director of the *Journal of Mechanical Engineering*, and an Associate Editor of the *Mechanism and Machine Theory* and the *International Journal of Mechanisms and Robotic Systems*.

Ming-Feng Ge (Member, IEEE) received the B.Eng. degree in automation and the Ph.D. degree in control theory and control engineering from the Huazhong University of Science and Technology, Wuhan, China, in 2008 and 2016, respectively.

He is currently an Associate Professor with the School of Mechanical Engineering and Electronic Information, China University of Geosciences, Wuhan. His current research interests include networked robotic systems, formation tracking, and multiagent networks.